SAND--88-3049C

CONF-8904246--4

DE89 010228

A MATHEMATICAL MODEL OF THE GAS-PHASE AND SURFACE CHEMISTRY IN GaAs MOCVD

MICHAEL E. COLTRIN* AND ROBERT J. KEE**
*Sandia National Laboratories, Albuquerque, NM 87185
**Sandia National Laboratories, Livermore, CA 94550

ABSTRACT

This paper presents a detailed mathematical model of the coupled gas-phase chemistry, surface chemistry, and fluid mechanics in the MOCVD of GaAs from trimethylgallium and arsine in a rotating-disk reactor. The model predicts steady-state deposition rates as a function of susceptor temperature and partial pressure of the reactants. Rate constants in the model have been adjusted to match experimental deposition rates from the literature.

INTRODUCTION

Computer modeling of the chemical vapor deposition process has been the subject of much work in this decade (see, for example, extensive reviews in Refs. [1,2]). Accurate computer models can be used to understand the complicated heat and mass transport leading to deposition. Ideally, such models can be used in the design phase of reactor development to address issues such as deposition uniformity and rate.

Previously, we have developed detailed computer models of the coupled gas-phase fluid flow and chemical kinetics in the deposition of Si from SiH_4 in boundary-layer flow [3,4] and for the infinite-radius rotating disk reactor [5]. Detailed predictions of the models compared well with *in situ* laser-based measurements of chemical species density profiles [6,7]. Our previous models contained a relatively simple treatment of the surface chemistry in the Si CVD system, i.e., boundary conditions on the concentrations of gas-phase species (sticking coefficients).

In the MOCVD of GaAs from trimethylgallium (TMG) and arsine (AsH_3), details of the surface chemistry are believed to dominate the deposition process [8]. Computer modeling of this system is considerably more challenging because much less is known of the fundamental surface (and gas-phase) kinetics than in the SiH_4 system. In this paper we describe our first attempts to develop a detailed model of the coupled surface chemistry, gas-phase chemistry, and fluid flow in GaAs MOCVD. Taking advantage of a similarity transformation, we use a simple one-dimensional model of an infinite-radius rotating disk [5,9]. A similar modeling effort was recently published by Tirtowidjojo and Pollard [10], who considered 232 gas-phase and 115 surface reactions for GaAs MOCVD in an impinging-jet reactor. The level of detail in our chemistry treatment is considerably simpler than in Ref. [10].

DEFINING EQUATIONS

The model solves for the coupled surface chemistry, gas-phase chemistry, and fluid flow in a rotating-disk reactor. We use the von Karman similarity transformation which results in a set of coupled, one-dimensional, ordinary differential equations, which are solved as a boundary-value problem [5,9]. The simplicity of the one-dimensional equations allows consideration of complex gas-phase and surface chemistry, at modest computational effort.

The equations defining the model are as follows:

$$\frac{du}{dx} + 2V + \frac{u}{\rho}\frac{d\rho}{dx} = 0 \qquad (1)$$

$$\frac{d}{dx}\left(\mu\frac{dV}{dx}\right) - \rho u\frac{dV}{dx} - \rho(V^2 - W^2) = 0 \tag{2}$$

$$\frac{d}{dx}\left(\mu\frac{dW}{dx}\right) - \rho u\frac{dW}{dx} - 2\rho VW = 0 \tag{3}$$

$$\frac{d}{dx}\left(\lambda\frac{dT}{dx}\right) - \rho c_p u\frac{dT}{dx} - \sum_{k=1}^{K_g}\left(c_{p_k}\rho Y_k V_k\frac{dT}{dx} + \dot{\omega}_k h_k\right) = 0 \tag{4}$$

$$\frac{d\rho Y_k V_k}{dx} + \rho u\frac{dY_k}{dx} - M_k\dot{\omega}_k = 0 \quad (k = 1, K_g - 1) \tag{5}$$

Equations (1)-(4) are the mixture continuity, radial momentum, circumferential momentum, and thermal energy equations, respectively. Equation (5) is a species continuity equation, for all but one of the K_g gas-phase species. (The last species concentration is found by ensuring that the mass fractions sum to one.)

In these equations the independent variable x is the distance normal to the disk surface. The dependent variables are the velocities, the temperature T, and the species mass fractions Y_k. The axial velocity is u, and the radial and circumferential velocities are scaled by the radius as $V = v/r$ and $W = w/r$. The diffusion velocities are given by:

$$V_k = \frac{1}{X_k\overline{M}}\sum_{j=1}^{K_g} M_j D_{kj}\frac{dX_j}{dx} - \frac{D_k^T}{\rho Y_k}\frac{1}{T}\frac{dT}{dx}. \tag{7}$$

In addition, we solve an equation stating that the time-derivative of the surface site fraction is zero for all K_s surface species. More details on the derivation of the equations and their method of solution are given in Ref. [5].

SURFACE REACTION MECHANISM

Little is known of the kinetics of elementary surface reactions in this system. In this preliminary work, we began by constructing a moderately-detailed surface mechanism (20 reactions) with estimated rate expressions for each reaction. Rate constants in the mechanism were optimized and reactions were added or deleted to match experimental deposition rates [8] over the temperature range 450 to 1050°. The reaction mechanism used in our work is given in Table I. Even though we do not represent this mechanism to be unique or complete, it does provide a reasonable description of GaAs deposition over this temperature range.

Reactions S1-S6 are adsorption reactions, assumed to proceed with near unit probability. Reactions S7-S9 are for production of gas-phase CH_4 from the reaction of a surface Ga-methyl species with surface AsH. The activation energy of S8 was set much lower than for the other two, in accord with the widely held belief that the second Ga-methyl bond is the easiest to break. Reactions S10-S14 are desorption reactions. The activation energies were set to increase monotonically as successive methyl groups are removed from the Ga species, in the belief that these species are able to form successively stonger bonds with the surface. The activation energy of S14 is in accord with the heat of vaporization of metallic Ga.

Reactions S15 and S16 are surface decomposition reactions, and S17 and S18 are recombinative desorption reactions. Rate parameters for these four reactions were freely adjusted, although the activation energy for S15 is in accord with preliminary temperature-programmed desorption results of Creighton [11]. Reactions S19-S22 describe rapid exchange of methyl radicals between surface Ga species, which is another result possibly suggested by the work of Creighton [11].

GAS-PHASE REACTION MECHANISM

The gas-phase reaction mechanism included in our model is given in Table II. The form of the modified Arrhenius expression for the rate constant is

$$k = AT^{\beta} \exp(-E/RT). \tag{8}$$

Rate constants for the reactions of hydrocarbon species, reactions G1 through G9, were taken from the combustion literature [12-16]. The only gas-phase reactions of gallium-containing or arsenic-containing species are reactions G10 and G11, the demethylation of trimethyl- and dimethylgallium, respectively. Rate constants for these two reactions were taken from Jacko and Price [17]. Thermochemical data for the gallium-containing and asenic-containing species were taken from the work of Tirtowidjojo and Pollard [18].

The pressure dependence of the rate constants is taken into account for reactions G1, G2, and G7. For these reactions, Arrhenius parameters are also given for the low-pressure limit. Two limits are connected either with a Lindemann form for reactions G2 and G7, or by a Troe form (see Refs. [12,19] for details) for reaction G1.

DEPOSITION RATES

Figure 1 presents deposition rates as a function of susceptor temperature predicted by the model for the following conditions: 1 atm H_2 carrier, 1.8×10^{-4} atm TMG, 3.3×10^{-3} atm AsH_3, 1000 rpm rotation rate. The surface-reaction rate constants were optimized to match experimental deposition rates [8]. The model matches the high activation energy for deposition at low temperature (kinetic-limited behavior), the transition to a region of small activation energy between about 600 and 850° (transport-limited behavior), and a strong negative temperature dependence above 850° (desorption controlled) exhibited experimentally [8].

In agreement with experiment [8], Fig. 2 shows that the model predicts deposition rates that are sublinear with respect to TMG partial pressure at low temperatures (compare with Figs. 2-4 of Ref. [8]). The calculated deposition rate is linear with respect to TMG at 700° and 1000°. The sublinear behavior at 500° is easy to understand by examining the predicted surface coverage as a function of TMG partial pressure, shown in Fig. 3. At low TMG partial pressure, the surface is covered with the arsenic species As and AsH. As more TMG is added to the inlet stream, the surface becomes filled with TMG and $GaCH_3$ (MMG) because the deposition reactions proceed very slowly. Thus, the deposition rate saturates due to the site-blockage of the gallium species.

At all temperatures the calculated deposition is weakly dependent on the arsine partial pressure, as illustrated in Fig. 4. (Again, these results may be compared with Figs. 2-4 of Ref. [8]).

DISCUSSION

In addition to deposition rates, the model also predicts concentration as a function of height above the disk for 13 gas-phase species, and site fractions for 7 surface species. These detailed predictions will not be discussed here, due to space limitations. However, we wish to conclude with a general discussion of the important deposition steps as suggested by our preliminary modeling work.

In our modeling, adsorption of TMG (reaction S2) is followed by rapid exchange of methyl groups (S19 and S21), producing three surface MMG species for each source molecule of TMG. Arsine is adsorbed (S1), followed by loss of H_2, to produce surface

AsH (S16). The final chemical step is to eliminate carbon via the production of CH_4 (S9). Note, however, that the simple 6-step scheme mentioned here requires three arsine source molecules for each source molecule of TMG. Therefore, in order to maintain the surface stoichiometry it is important that some of the surface As produced is desorbed (S17).

This simple reaction scheme is consistent with the spectroscopic finding [20] that replacing H_2 carrier with D_2 would produce no CH_3D. It provides a simple explanation for the need for excess AsH_3 usually used in MOCVD. It is consistent with preliminary TPD work suggesting rapid methyl exchange on the surface [11]. Of course, what is critically needed are independent measurements of some of the fundamental decompositon steps to test and to improve the assumptions in numerical models such as these. As such fundamental studies become available, our understanding of the MOCVD process will proceed.

ACKNOWLEDGEMENTS

We would like to thank Randy Creighton, Kevin Killeen, and Greg Evans for many helpful discussions. This work was performed at Sandia National Laboratories, supported by the U.S. Department of Energy, Office of Basic Energy Sciences under contract No.DE-AC04-76DP00789.

REFERENCES

1. D. W. Hess, K. F. Jensen, and T. J. Anderson, *Rev. Chem. Eng.*, **3**, 97 (1985).
2. K. F. Jensen, *Chem. Eng. Sci.*, **42**, 923 (1987).
3. M. E. Coltrin, R. J. Kee, and J. A. Miller, *J. Electrochem. Soc.* **131**, 425 (1984).
4. M. E. Coltrin, R. J. Kee, and J. A. Miller, *J. Electrochem. Soc.* **133**, 1206 (1986).
5. M. E. Coltrin, R. J. Kee, and G. H. Evans, *J. Electrochem. Soc.*, **136**, 819 (1989).
6. W. G. Breiland, M. E. Coltrin, and P. Ho, *J. Appl. Phys.* **59**, 3267 (1986).
7. W. G. Breiland, P. Ho, and M. E. Coltrin, *J. Appl. Phys.* **60**, 1505 (1986).
8. D. H. Reep and S. K. Ghandhi, *J. Electrochem. Soc.*, **130**, 675 (1983).
9. R. Pollard, and J. Newman, *J. Electrochem. Soc.* **127**, 744 (1980).
10. M. Tirtowidjojo and R. Pollard, *J. Cryst. Growth*, **93**, 108 (1988).
11. J. R. Creighton, private communication.
12. A. F. Wagner and D. M. Wardlaw, *J. Phys. Chem.*, **92**, 2462 (1988).
13. T. C. Clark and J. E. Dove, *Can. J. Chem.*, **51**, 2147 (1973).
14. J. Warnatz, *Combustion Chemistry*, (W. C. Gardiner, Ed.), Springer, 1984.
15. G. Dixon-Lewis, *Phil. Trans. R. Soc. Lond.*, **A303**, 181 (1981).
16. P. Glarborg, J. A. Miller, and R. J. Kee, *Combust. and Flame*, **65**, 177 (1986).
17. M. G. Jacko and S. J. W. Price, *Can. J. Phys.*, **41**, 1560 (1963).
18. M. Tirtowidjojo and R. Pollard, *J. Cryst. Growth*, **77**, 200 (1986).
19. R. G. Gilbert, K. Luther, and J. Troe, *Ber. Bunsenges. Phys. Chem.*, **87**, 161 (1983).
20. C. A. Larsen, N. I. Buchan, and G. B. Stringfellow, *Appl. Phys. Lett.*, **52**, 480 (1988).

DISCLAIMER

Table I: Surface reaction mechanism

	Reaction	A^a	E^a
S1	$AsH_3 + Ga(s) \longrightarrow AsH_3(s) + Ga(d)$	4.0×10^{11}	0.
S2	$TMG + As(s) \longrightarrow TMG(s) + As(d)$	4.0×10^{11}	0.
S3	$DMG + As(s) \longrightarrow DMG(s) + As(d)$	4.0×10^{11}	0.
S4	$MMG + As(s) \longrightarrow MMG(s) + As(d)$	4.0×10^{11}	0.
S5	$Ga + As(s) \longrightarrow Ga(s) + As(d)$	4.0×10^{11}	0.
S6	$As_2 + 2Ga(s) \longrightarrow 2As(s) + Ga(d)$	4.0×10^{20}	0.
S7	$TMG(s) + AsH(s) \longrightarrow DMG(s) + As(s) + CH_4$	1.0×10^{23}	50000.
S8	$DMG(s) + AsH(s) \longrightarrow MMG(s) + As(s) + CH_4$	8.0×10^{19}	20000.
S9	$MMG(s) + AsH(s) \longrightarrow Ga(s) + As(s) + CH_4$	1.0×10^{23}	50000.
S10	$AsH_3(s) + Ga(d) \longrightarrow AsH_3 + Ga(s)$	1.0×10^{11}	25000.
S11	$TMG(s) + As(d) \longrightarrow TMG + As(s)$	1.0×10^{11}	15000.
S12	$DMG(s) + As(d) \longrightarrow DMG + As(s)$	1.0×10^{11}	25000.
S13	$MMG(s) + As(d) \longrightarrow MMG + As(s)$	1.0×10^{11}	40000.
S14	$Ga(s) + As(d) \longrightarrow Ga + As(s)$	1.0×10^{11}	65000.
S15	$MMG(s) \longrightarrow Ga(s) + CH_3$	1.0×10^{13}	43000.
S16	$AsH_3(s) \longrightarrow AsH(s) + H_2$	1.0×10^{13}	25000.
S17	$2As(s) + 2Ga(d) \longrightarrow As_2 + 2Ga(s)$	1.7×10^{22}	40000.
S18	$2AsH(s) \longrightarrow 2As(s) + H_2$	6.0×10^{23}	35000.
S19	$TMG(s) + Ga(s) \longrightarrow DMG(s) + MMG(s)$	6.0×10^{23}	10000.
S20	$DMG(s) + MMG(s) \longrightarrow TMG(s) + Ga(s)$	6.0×10^{23}	20000.
S21	$DMG(s) + Ga(s) \longrightarrow 2MMG(s)$	6.0×10^{23}	10000.
S22	$2MMG(s) \longrightarrow DMG(s) + Ga(s)$	6.0×10^{23}	20000.

[a] Arrhenius parameters; units are in terms of mols, cm, sec, and cal/mol.

Table II: Gas-phase reaction mechanism

	Reaction	A^a	β^a	E^a
G1	$CH_3 + CH_3 + M \longleftrightarrow C_2H_6 + M$	9.03×10^{16}	-1.18	654.
	(H_2 enhancement = 2.0)	3.18×10^{41}[b]	-7.03[b]	2762.[b]
		0.6041[c]	6927.[c]	132.[c]
G2	$CH_3 + H + M \longleftrightarrow CH_4 + M$	6.0×10^{16}	-1.0	0.0
	(H_2 enhancement = 2.0)	8.0×10^{26}[b]	-3.0[b]	0.0[b]
G3	$CH_4 + H \longleftrightarrow CH_3 + H_2$	2.2×10^{4}	3.0	8750.
G4	$C_2H_6 + CH_3 \longleftrightarrow C_2H_5 + CH_4$	5.5×10^{-1}	4.0	8300.
G5	$C_2H_6 + H \longleftrightarrow C_2H_5 + H_2$	5.4×10^{2}	3.5	5210.
G6	$H + C_2H_4 + M \longleftrightarrow C_2H_5 + M$	2.21×10^{13}	0.0	2066.
	(H_2 enhancement = 2.0)	6.37×10^{27}[b]	-2.76[b]	-54.[b]
G7	$C_2H_5 + H \longleftrightarrow CH_3 + CH_3$	1.0×10^{14}	0.0	0.
G8	$H + H + M \longleftrightarrow H_2 + M$	1.0×10^{18}	-1.0	0.
G9	$H + H + H_2 \longleftrightarrow H_2 + H_2$	9.2×10^{16}	-0.6	0.
G10	$TMG \longleftrightarrow DMG + CH_3$	3.47×10^{15}	0.0	59500.
G11	$DMG \longleftrightarrow MMG + CH_3$	8.71×10^{7}	0.0	35410.

[a] Arrhenius parameters; units are in terms of mols, cm, sec, and cal/mol.

[b] Low pressure limit (see text).

[c] Troe centering parameters, a, T^{***}, and T^{*}, respectively (see Refs. [12,19]).

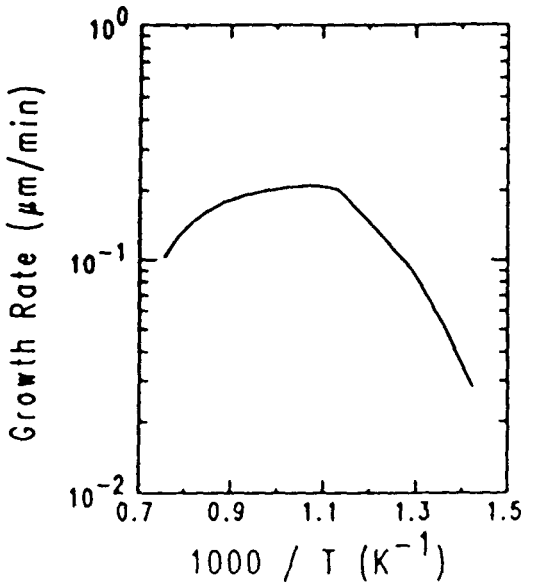

FIG. 1

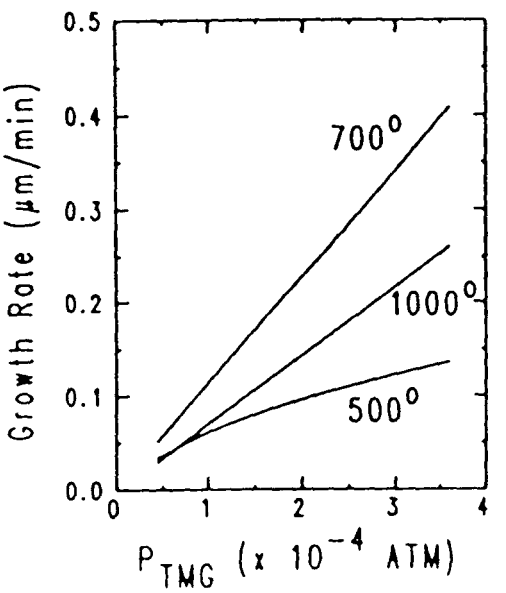

FIG. 2

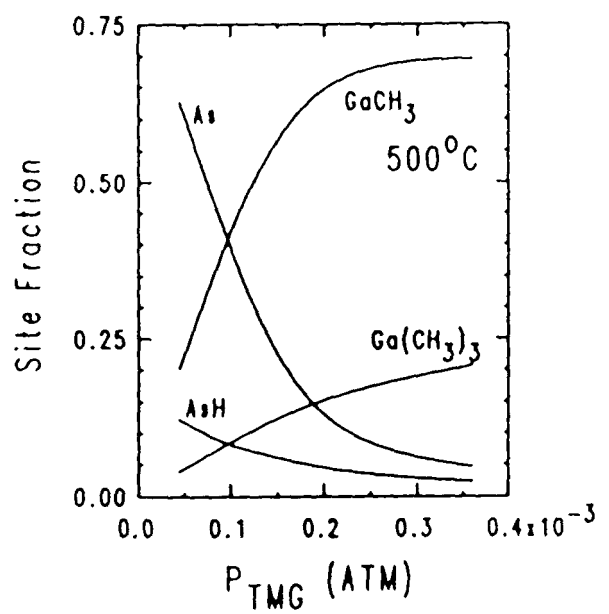

FIG. 3

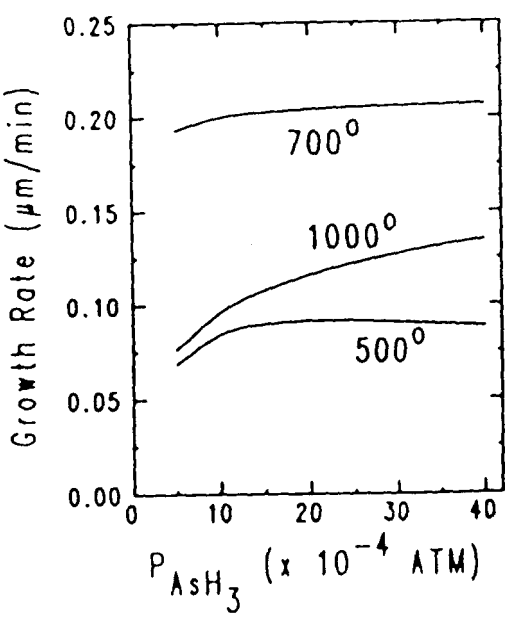

FIG. 4